PHYSICAL REVIEW D VOLUME 10, NUMBER 3 1 AUGUST 1974

Glauber-Deck model for 3π production on nuclei*

R. T. Cutler
Department of Physics, University of Illinois, Urbana, Illinois 61801
(Received 19 February 1974; revised manuscript received 13 May 1974)

A Glauber theory is developed for the reaction $\pi^- A \to \pi^+\pi^-\pi^- A$, where A is a nucleus, using a Reggeized Deck amplitude for 3π production on a nucleon. A simple absorption amplitude for the 3π system is used in which the pions are assumed not to interact. The resulting amplitude is calculated for carbon at 15.1 GeV/c, using a Monte Carlo approach. An alternative absorption scheme is discussed, and a multi–impact-parameter model proposed. The multi–impact-parameter model is found to result in cross sections practically identical to computationally simpler models. The reaction $\pi^- C \to \pi^+\pi^-\pi^- C^*_{4.44}$ is also calculated using an effective one-particle excitation parametrization, and the results are compared to experimental data at 6 GeV/c.

I. INTRODUCTION

The idea that one may learn about the reaction $\pi^- p \to \pi^+\pi^-\pi^- p$ by studying 3π production on nuclei is a familiar one. In particular, one expects to be able to distinguish[1] between a kinematic enhancement like the Deck effect and a true 3π resonance by extracting the cross section, $\sigma_{3\pi}$, for interaction between the 3π system and a nucleon. The experimental $\pi^- A \to \pi^+\pi^-\pi^- A$ data[2] have been analyzed using a simple multiple-scattering formalism, yielding[3] $\sigma_{3\pi} \approx \sigma_\pi \approx 25$ mb. This low a value of $\sigma_{3\pi}$ has been considered to be inconsistent[4,5] with production of the A_1 by a kinematic enhancement where final-state interactions are negligible.

On the other hand, spin-parity fits to $\pi p \to 3\pi p$ have shown[6] that the A_1 bump, which is primarily a $J^P = 1^+$ state, does not have the rapidly varying phase that one would expect were it a true resonance. Furthermore, recent Reggeized Deck calculations[7] of $\pi p \to 3\pi p$ have achieved very respectable detailed agreement with experiment without the use of any free parameters.

Can the Deck model of 3π production on a nucleon be reconciled with the nuclear data? Several models have been proposed[8] which will give low 3π absorption without the formation of a resonant state. These models typically depart significantly from conventional multiple-scattering theory, and the possibility of learning about 3π production on nucleons may be lost. This paper will attempt to answer the question of whether such drastic measures can be avoided by amalgamating Glauber multiple-diffraction theory with a Deck amplitude for 3π production on a nucleon. The Deck amplitude will be realistic (to the extent that the calculations of Ref. 7 agree with experiment) in all seven nontrivial production variables.

The Glauber-Deck amplitude will be developed using well-known methods in Sec. II. A Monte Carlo technique will be used in Sec. III to calculate cross sections for the specific reaction $\pi^- C \to \pi^+\pi^-\pi^- C$ at 15.1 GeV/c lab momentum, which will be compared with the experimental data[2,3] at this energy. The result of this detailed calculation agrees with the simpler analysis of Ref. 3, in that a model with a final state of three independent pions is inconsistent with the data. Considering the effect of ρ production on the absorption has very little effect on the cross section. A multi–impact-parameter model will be proposed in Sec. IV and shown to yield results practically identical to the computationally much simpler methods of Secs. II and III.

The methods of preceding sections will be used in Sec. V to analyze the reaction $\pi^- C \to \pi^+\pi^-\pi^- C^*$, where C^* is the $J^P = 2^+$ excited state of carbon at 4.44 MeV. An Illinois group has observed this reaction[9] at 5 GeV/c by identifying the characteristic γ emission of the nuclear final state. In a previous article[10] (hereafter referred to as I) a Reggeized Deck model was directly applied to $\pi C \to 3\pi C^*$ (and also $\pi C \to 3\pi C$), resulting in a pleasing agreement with experiment for the shapes of the $M_{3\pi}$ and t distributions. However, this approach has two unattractive features: It ignores the known structure of the nucleus, treating carbon as an elementary particle, and it does not seem to treat correctly the absorption of the outgoing 3π system.

In Sec. V, the Glauber-Deck model will be combined with a simple parametrization for the excitation of the nucleus to derive an amplitude for $\pi C \to 3\pi C^*$. The excitation form factor will be fitted to experimental results of $\pi C \to \pi C^*$, and the reaction $\pi C \to 3\pi C^*$ will be calculated and compared with experiment in Sec. VI. The data available at this time will be shown to be consistent with $\sigma_{3\pi} \approx 25$ mb, and inconsistent with an independent-particle final state.

II. PION PRODUCTION IN GLAUBER THEORY; A SIMPLE MODEL

The Glauber theory of multiple diffraction[11] has been quite successful in calculating reactions like $\pi A \to \pi A$. To review briefly, the Glauber amplitude for elastic scattering at high energy and small momentum transfer is

$$F_{\pi A}(\vec{q}) = \frac{ik}{2\pi} \int d^2b \left(\prod_{k=1}^{A} d^3r_k \right) e^{i\vec{q}\cdot\vec{b}} |u(\vec{r}_1, \ldots, \vec{r}_A)|^2 \times \left\{ 1 - \prod_{l=1}^{A} [1 - \gamma(\vec{b} - \vec{s}_l)] \right\}, \quad (1)$$

$$\gamma(b) \equiv \frac{1}{2\pi i k} \int f_{\pi N}(\vec{q}) e^{-i\vec{q}\cdot\vec{b}} d^2q, \quad (2)$$

where b is an impact parameter, $\vec{r}_k = (\vec{s}_k, z_k)$ are the coordinates of the kth nucleon, and $\vec{q}$ is the momentum transfer, $t = -q^2$. If one makes the approximations, valid for large nuclei and used throughout this report,

$$|u(\vec{r}_1, \ldots, \vec{r}_A)|^2 \cong \prod_{m=1}^{A} \rho(r_m), \quad (3)$$

$$\begin{aligned} \int \gamma(\vec{b} - \vec{s}) \rho(\vec{s}, z) d^2s\, dz &\cong \int \gamma(s) d^2s \int \rho(\vec{b}, z) dz \\ &= \frac{2\pi i}{k} f(0) \frac{T(b)}{A} \\ &= \frac{\sigma(1 - i\alpha)}{2} \frac{T(b)}{A}, \end{aligned} \quad (4)$$

with

$$\begin{aligned} T(b) &\equiv A \int_{-\infty}^{\infty} \rho(b, z)\, dz, \\ \alpha &\equiv \frac{\text{Re} f(0)}{\text{Im} f(0)}, \\ 1 &= \int d^3r \rho(r), \\ \sigma' &\equiv \sigma(1 - i\alpha), \end{aligned} \quad (5)$$

and uses

$$\left(1 - \frac{x}{A}\right)^A \cong e^{-x}, \quad (6)$$

the scattering amplitude becomes

$$F_{\pi A}(q) = \frac{ik}{2\pi} \int d^2b\, e^{i\vec{q}\cdot\vec{b}} \left(1 - e^{-(\sigma'/2)T(b)}\right). \quad (7)$$

Note that σ, σ', $f(q)$, and α all refer to $\pi N \to \pi N$, with N a nucleon. This amplitude results in t distributions determined by the size of the entire nucleus, since the scattering from the nucleons is summed coherently. The incoherent process, where the final state of the nucleus is summed over, will not be considered in this paper, since it can be distinguished in the experimental data from the coherent contribution by its t distribution; it is, of course, absent in the case where C* is observed.

Kölbig and Margolis[12] have suggested an extension of Glauber theory to reactions of the type $aA \to bA$, where a and b are different particles (e.g., $a = \pi$, $b = \rho$). They assume that $\sigma_{ab} \ll (\sigma_a$ and $\sigma_b)$, where σ_{ab} is the cross section for $aN \to bN$, and $\sigma_a(\sigma_b)$ is the total cross section for particle $a(b)$ on a nucleon, and thus they treat the production of b in first order.

The theory reported here is similar to that of Kölbig and Margolis, except for two assumptions designed to treat the 3π production on nucleons by a Deck mechanism:

(1) A Deck amplitude[7] is used for $\pi N \to 3\pi N$.

(2) The 3π system is assumed to be absorbed as if it were three noninteracting pions, all at the same impact parameter. Alternatives to this assumption will be discussed in Secs. III and IV.

The starting point for this calculation is, then,

$$F_{3\pi C} = \frac{ik}{2\pi} \sum_{j=1}^{A} \int d^2b \left(\prod_{k=1}^{A} d^3r_k \right) e^{i\vec{q}\cdot\vec{b}} |u(\vec{r}_1, \ldots, \vec{r}_A)|^2 \Gamma_{\pi,3\pi}(\vec{b} - \vec{s}_j) e^{iq_L z_j} \times \prod_{z_i < z_j} [1 - \gamma(\vec{b} - \vec{s}_i)] \prod_{z_l > z_j} [1 - \Gamma_{3\pi,3\pi}(\vec{b} - \vec{s}_l)], \quad (8)$$

with

$$1 - \Gamma_{3\pi,3\pi}(\vec{b}) = [1 - \gamma(\vec{b})]^3, \quad (9)$$

$$\Gamma_{\pi,3\pi}(b) = \frac{1}{2\pi i k} \int f_{3\pi N}(q) e^{-i\vec{q}\cdot\vec{b}} d^2q. \quad (10)$$

The factor $e^{iq_L z_j}$ in (8), where $q_L \equiv \vec{q} \cdot \hat{z}$, is not present in similar formulas of Ref. 12 (Kölbig and Margolis treat $q_L \neq 0$ in the optical approximation). Equation (8) may be derived by carefully keeping track of the phase accumulated by the π

and the (3π) system as they propagate from nucleon to nucleon through the nucleus (see Appendix). The quantity q_L will be assumed to be small for $\pi C \to 3\pi C$, since high-energy experimental data are available for this reaction. As can be seen in the optical model calculations of Ref. 12, the effect of a small q_L can be approximated by the substitution $q_\perp \to \sqrt{-t}$ in the $q_L = 0$ formulas. This is the approach that will be taken here.

In order to use a Deck amplitude for $\Gamma_{\pi,3\pi}$, $f_{3\pi N}$ must be converted to an invariant amplitude. The nucleon will be treated as spinless in the following, and all momenta and angles will be in the lab system unless otherwise specified. The cross section for $\pi N \to 3\pi N$ is

$$d\sigma_{3\pi N} = \frac{1}{(2\pi)^8 2^{10} (p_\pi M_N)^2} \, |\mathfrak{M}_{3\pi N}|^2 \, d^8\tau , \tag{11}$$

with

$$d^8\tau = \frac{dM_{3\pi}}{M_{3\pi}} \, dt \, d\alpha d\cos\beta \, d\gamma \, ds_1 \, ds_2 \, d\phi \equiv dt \, d\phi d^6\tau , \tag{12}$$

where t is the momentum transfer to the 3π system, α, $\cos\beta$, and γ are Euler angles describing the orientation of the three pions in the 3π center-of-mass system, s_1 and s_2 are the Dalitz-plot variables, and ϕ is the azimuthal angle of the 3π system. Then, changing variables from t to the production angles of the 3π system, one finds

$$\begin{aligned} d\sigma_{3\pi N} &= \left(\frac{1}{(2\pi)^4 2^5 p_\pi M_N}\right)^2 2p_\pi \, p_{3\pi} |\mathfrak{M}_{3\pi N}|^2 \, d\Omega_L \, d^6\tau \\ &= |f_{3\pi N}|^2 \, d\Omega_L \, d^6\tau , \end{aligned} \tag{13}$$

and so one has

$$\Gamma_{\pi,3\pi}(\vec{b}) = \frac{1}{2\pi i k} \frac{(2p_\pi p_{3\pi})^{1/2}}{(2\pi)^4 2^5 p_\pi M_N} \times \int \mathfrak{M}_{3\pi N}(q) \, e^{-i\vec{q}\cdot\vec{b}} \, d^2 q . \tag{14}$$

A Deck amplitude[7,10] is now used for $\mathfrak{M}_{3\pi N}$:

$$\mathfrak{M}_{3\pi N} = \sum_{\text{diagrams}} \mathfrak{M}_{\pi\pi} \, \mathcal{R} \, \mathfrak{M}_{\pi N} , \tag{15}$$

$$\begin{aligned} \mathcal{R} &= \left(\frac{s_R - u_R}{2s_0}\right)^{\alpha_\pi(t_R)} e^{-i\pi\alpha_\pi(t_R)/2} \frac{1}{t_R - \mu^2} , \\ \alpha_\pi(t_R) &= t_R - \mu^2 , \\ s_0 &= 1 \text{ GeV} . \end{aligned} \tag{16}$$

The diagrams summed over and conventions of notation are illustrated in Fig. 1. A fit to experimental data, discussed in Ref. 7, is used for $\mathfrak{M}_{\pi\pi}$. Noting that

$$\gamma(b) = \frac{-i}{(2\pi)^2 2^2 p^{\text{c.m.}}_{\pi N} M_{\pi N}} \int \mathfrak{M}_{\pi N}(q) \, e^{-i\vec{q}\cdot\vec{b}} \, d^2 q , \tag{17}$$

where $p^{\text{c.m.}}_{\pi N}$ refers to the c.m. system of the lower (πN) vertex, one finds

$$\frac{ik}{2\pi} \Gamma_{\pi,3\pi}(b) = \frac{i\sqrt{2}}{(2\pi)^4 2^3} \left(\frac{p_{3\pi}}{p_\pi}\right)^{1/2} \frac{p^{\text{c.m.}}_{\pi N} M_{\pi N}}{M_N} \times \sum_{\text{diagrams}} \mathfrak{M}_{\pi\pi} \, \mathcal{R} \gamma(b) . \tag{18}$$

It has been assumed that $\sigma(\pi N \to \pi N)$ is a constant in the range of $M_{\pi N}$ of interest, and this model is thus similar in this respect to FIT 3 in I.

If one approximates the 3π absorption amplitude (9) by $(1-\gamma)^3 \cong 1 - 3\gamma$, then $F_{3\pi C}$ has the same form as that of Ref. 12, except that an explicit production mechanism is included. In this case $\sigma_{3\pi}/\sigma_\pi = 3$, which disagrees with the experimental value[3] of 1.0 to 1.2. However, the higher-order terms may be evaluated by employing an approximate form for $f_{\pi N}(q)$ and using (2)–(5). If one writes

$$\begin{aligned} 1 - \frac{\sigma' T(b)}{2A} \Delta &\equiv \int [1 - \gamma(\vec{b} - \vec{s})]^3 \rho(s, z) \, d^2 s \, dz , \\ \sigma' &\equiv (1 - i\alpha)\sigma , \end{aligned} \tag{19}$$

and uses

$$f_{\pi N} = \frac{i\sigma' k}{4\pi} e^{-aq^2/2} , \tag{20}$$

then one finds

$$\Delta = 3 - \frac{3\sigma'}{8\pi a} + \frac{(\sigma')^2}{48\pi^2 a^2} . \tag{21}$$

The real part of Δ may be identified with $\sigma_{3\pi}/\sigma_\pi$ of the first-order theory, and interpreted as an effective number of pions in the outgoing system. For $\sigma = 25$ mb, $\alpha = -0.2$, and $a = 8$ GeV^{-2}, one finds $\Delta = 2.17 - 0.14i$. This reduction of effective-pion number by considering nonlinear terms in γ is called "shadowing" in Ref. 5. The 3π production amplitude (8) now becomes, using (18), (19), and (6) and summing the series as in Ref. 12,

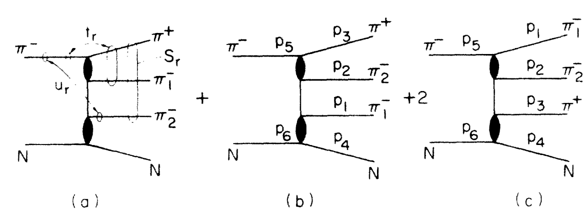

FIG. 1. Diagrams calculated in Deck model.

$$F_{3\pi C}(\tau) = \frac{i\sqrt{2}}{(2\pi)^4 2^3}\left(\frac{p_{3\pi}}{p_\pi}\right)^{1/2} \sum_{\text{diagrams}} \left(\frac{p_{\pi N}^{\text{c.m.}} M_{\pi N}}{M_N}\right) \times \mathfrak{M}_{\pi\pi} \mathfrak{R} Z(t), \quad (22)$$

$$Z(-q^2) = \int d^2b \left(\frac{e^{\sigma' T(b)/2} - e^{-\Delta\sigma' T(b)/2}}{\Delta - 1}\right) e^{i\vec{q}\cdot\vec{b}}.$$

The cross section is then given by

$$d\sigma = \frac{1}{(2\pi)^8 2^6}\left|\sum_{\text{diagrams}}\left(\frac{p_{\pi N}^{\text{c.m.}} M_{\pi N}}{p_\pi M_N}\right)\mathfrak{M}_{\pi\pi}\mathfrak{R} Z(t)\right|^2 d^8\tau. \quad (23)$$

III. CALCULATION OF $\pi^- C \to \pi^+\pi^-\pi^- C$

The primary t dependence of $F_{3\pi C}$ may be displayed by calculating $Z(t)$. $T(b)$ is calculated from a modified Gaussian wave function for carbon[13]

$$\rho(r) = \frac{1}{\rho_0}\left(1 + \alpha\frac{r^2}{r_0^2}\right) e^{-r^2/r_0^2}, \quad (24)$$

$$\rho_0 = \pi^{3/2} r_0^3 (1 + \tfrac{3}{2}\alpha),$$

with $\alpha = 1.12$ and $r_0 = 1.71$ fm. The integration is performed numerically and the results are shown in Fig. 2. If the $\Delta = 1.1$ curve is identified with experiment, shadowing is seen to remove a part of the discrepancy between the simplest theory, $\Delta = 3$, and experiment.

As in I, a Monte Carlo approach is used to display the full content of (23). The Monte Carlo calculation generates a random sample of 3π events which are distributed according to $d\sigma/d^8\tau$. These events can be analyzed in exactly the same way one would treat experimental data. Events were generated in $M_{3\pi}$ bins of 100 MeV, from 0.8 to 2.0 GeV at incident pion momentum 15.1 GeV/c. Approximately 1500 events were generated in each bin at about 5% efficiency. The resulting $M_{3\pi}$ distribution is compared to experiment in Fig. 3. The theoretical $M_{3\pi}$ spectrum has been multiplied by 3.0, in order to make the peaks of the two curves coincide. The shape of the $M_{3\pi}$ spectrum is seen to be well predicted.

Figure 4 shows the theoretical and experimental distributions of coherent events in t', with $0.9 < M_{3\pi} < 1.9$ GeV. The incoherent contribution to the experiment has been approximated by $d\sigma_I/dt' = I_0 e^{bt'}$, with $I_0 = 8.45$ mb GeV^{-2} and $b = 8.53$ GeV^{-2}, and has been subtracted from the total experimental data. This incoherent cross section is a fit by eye to the data with $t' > 1.4$ GeV^2, as shown in Fig. 4, and should be considered an estimate. The resulting coherent cross section is, for $t' \gtrsim 0.05$ GeV^2, very sensitive to the incoherent fit. However, there does seem to be evidence for a dip in the experimental data at $t' \approx 0.075$ GeV^2, which (cf. Fig. 2) is consistent with $\Delta = 1.1$, as claimed in Ref. 3. The ratio between calculation and experiment is roughly the same as the ratio of curves (b) and (d) in Fig. 2. Evidently this detailed calculation has confirmed that the experimental data are consistent with $\Delta = 1.1$, and not with a model where the final-state pions interact independently.

The Monte Carlo calculation allows other distributions to be displayed, but there is little difference in most spectra between this calculation and those reported in I and Ref. 7. In particular,

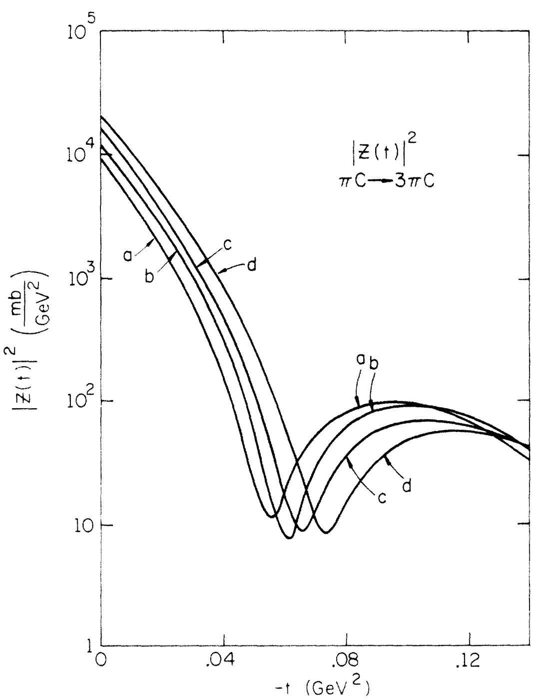

FIG. 2. $|Z(t)|^2$ for $\pi^- C \to \pi^+\pi^-\pi^- C$. (a) $\Delta = 3$, most naive theory. (b) $\Delta = 2.17 - 0.14i$, three noninteracting pions (SIM). (c) $\Delta = 1.68 - 0.06i$, 3π absorbed as $\pi\rho$. (d) $\Delta = 1.1$, approximates experiment.

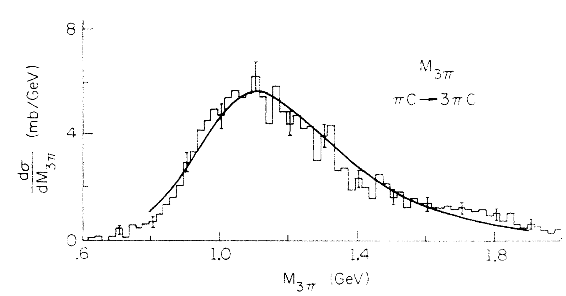

FIG. 3. 3π mass distribution for $\pi^- C \to \pi^+\pi^-\pi^- C$. Experimental curve is from Ref. 2. The theoretical curve has been multiplied by 3 to make the peaks coincide.

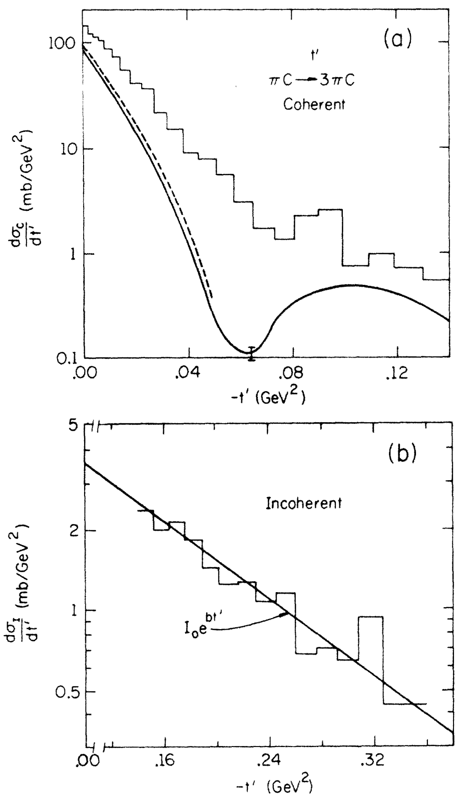

FIG. 4. Distribution in momentum transfer $t' = t - t_{min}$ for $\pi^- C \to \pi^+\pi^-\pi^- C$. (a) Coherent cross section, $d\sigma_C/dt' = d\sigma_{tot}/dt' - d\sigma_I/dt'$. The solid curve refers to the three-independent-pion model of Sec. II; the broken curve allows the 3π to be absorbed as $\pi\rho$. (b) Incoherent cross section, $d\sigma_I/dt'$. Experimental curves from Ref. 1.

the ρ band is very prominent, 56% of the Monte Carlo events having at least one $\pi^+\pi^-$ mass within 100 MeV of $M_\rho = 770$ MeV.

It may be argued that ρ production is so dominant that 3π absorption should be calculated as $\pi\rho$ absorption.[4,1] If the ρ-nucleon interaction[14] is approximated by $\sigma_{\rho N} = \sigma_{\pi N}$, then $1 - \Gamma_{3\pi,3\pi}(b) = [1-\gamma(b)]^2$, resulting in $\Delta = 1.68 - 0.06i$. Curve (c) in Fig. 2 shows $|Z(t)|^2$ for this value of Δ. A Monte Carlo calculation can now be done where the lower value of Δ is used for those events where the $\pi^+\pi^-$ from the upper vertex are in a rather wide ρ band, $670 < M_{\pi^+\pi^-} < 870$ MeV, and

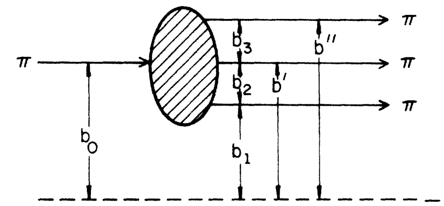

FIG. 5. Definition of various impact parameters with respect to an arbitrary reference axis. The top two pions are from the upper ($\pi\pi$) vertex; the lowest pion is from the lower (πN) vertex.

the higher value of Δ is used otherwise. (The ability to do this kind of calculation demonstrates the flexibility of a Monte Carlo approach.) Approximately 2500 events were generated in each $M_{3\pi}$ bin, and the resulting t' distribution for $0.9 < M_{3\pi} < 1.9$ GeV is shown in Fig. 4. For $t' \gtrsim 0.05$, the statistics of the Monte Carlo calculation are not good enough to cleanly separate the two theoretical curves. The effect of including $\pi\rho$ absorption is seen to be rather small.

IV. A MULTI-IMPACT-PARAMETER MODEL

It is possible to formulate a more complicated theory by removing the assumption that all three pions leave the nucleus with the same impact parameter. It seems plausible to assign different impact parameters $(\vec{b}_1, \vec{b}', \vec{b}'')$ to the produced pions, and another $(\vec{b}_0)$ to the incident pion, as shown in Fig. 5. The usual identification $l = kb + \frac{1}{2} \cong kb$, valid for $k \gg q$, along with the provision that the nucleus not change its spin, yields

$$k(\hat{z}\times\vec{b}_0) \cong k_1(\hat{z}\times\vec{b}_1) + k_2(\hat{z}\times\vec{b}') + k_3(\hat{z}\times\vec{b}''),$$

$$\vec{b}_0 \cong \frac{k_1\vec{b}_1 + k_2\vec{b}' + k_3\vec{b}''}{k}. \quad (25)$$

This model will be referred to as MIM (multi-impact model), and the model of Sec. II as SIM (single-impact model). It would seem that MIM is a more logical approach to a Deck calculation than SIM, since the latter is expressly formulated in Ref. 12 to describe the propagation of a resonance through nuclear matter. A straightforward extension of Glauber formalism to MIM, which can be derived by keeping track of the phases of each particle (see Appendix), is

$$\mathfrak{M}^{\text{MIM}}_{3\pi C} = \int d^2b_1\, d^2b_2\, d^2b_3\, e^{i(\vec{q}_1\cdot\vec{b}_1 + \vec{q}_2\cdot\vec{b}_2 + \vec{q}_3\cdot\vec{b}_3)}\, \tilde{\mathfrak{M}}^{\text{MIM}}_{3\pi C}(b_1, b_2, b_3),$$

$$\tilde{\mathfrak{M}}^{\text{MIM}}_{3\pi C} = \sum_{j=1}^{A} \int \prod_{k=1}^{A} d^3r_k\, |u(\vec{r}_1, \ldots, \vec{r}_A)|^2\, \mathfrak{M}_{\pi\pi}(b_3)\,\mathfrak{R}(b_2)\, \mathfrak{M}_{\pi N}(\vec{b}_1 - \vec{s}_j)\, e^{iq_L z_j}$$
$$\times \prod_{z_i < z_j} [1-\gamma(\vec{b}_0 - \vec{s}_i)] \prod_{z_l > z_j} [1-\gamma(\vec{b}_1 - \vec{s}_l)][1-\gamma(\vec{b}' - \vec{s}_l)][1-\gamma(\vec{b}'' - \vec{s}_l)], \quad (26)$$
$$\vec{b}_2 \equiv \vec{b}' - \vec{b}_1, \quad \vec{b}_3 \equiv \vec{b}'' - \vec{b}',$$

where $\vec{q}_i$ is the momentum transfer conjugate to $\vec{b}_i$ [note that $(\vec{q}_1, \vec{b}_1)$ were called $(\vec{q}, \vec{b})$ in earlier sections]. As in Sec. II, q_L will be assumed to be small, and $q_\perp \to \sqrt{-t}$ will be used in the $q=0$ formulas. The amplitudes $(\tilde{\mathfrak{M}}_{\pi\pi}, \tilde{\mathfrak{R}}, \tilde{\mathfrak{M}}_{\pi N})$ are Fourier transforms of $(\mathfrak{M}_{\pi\pi}, \mathfrak{R}, \mathfrak{M}_{\pi N})$. In particular,

$$\tilde{\mathfrak{M}}_{\pi N}(b) = \frac{1}{(2\pi)^2}\int \mathfrak{M}_{\pi N}(q)\, e^{-i\vec{q}\cdot\vec{b}}\, d^2q = 4i\, p_{\pi N}^{\text{c.m.}} M_{\pi N}\, \gamma(b)\,. \tag{27}$$

In order to evaluate (26), one uses (20) and (2)–(5) to find

$$\int \gamma(\vec{b}_1 - \vec{s})\,\gamma(\vec{b}_1 + \vec{b}_2 - \vec{s})\,\rho(\vec{s}, z)\, d^2s\, dz \cong \int \gamma(\vec{b}_1 - \vec{s})\,\gamma(\vec{b}_1 + \vec{b}_2 - \vec{s})\, d^2s \times \int \rho(\vec{b}_1 + \tfrac{1}{2}\vec{b}_2, z)\, dz \cong \frac{\sigma'}{16\pi a}\, e^{-b_2^2/4a}\, \frac{T(\vec{b}_1 + \frac{1}{2}\vec{b}_2)}{A}\,. \tag{28}$$

Dropping small terms involving the product of three γ factors for the outgoing pions, one finds

$$F_{3\pi C}^{\text{MIM}} = \frac{i\sqrt{2}}{(2\pi)^4\, 2^3}\left(\frac{p_{3\pi}}{p_\pi}\right)^{1/2} \sum_{\text{diagrams}} \left(\frac{p_{\pi N}^{\text{c.m.}} M_{\pi N}}{M_N}\right)\int d^2b_1\, d^2b_2\, d^2b_3\, e^{i(\vec{q}_1\cdot\vec{b}_1 + \vec{q}_2\cdot\vec{b}_2 + \vec{q}_3\cdot\vec{b}_3)}\, \tilde{W}(b_1, b_2, b_3)\,, \tag{29}$$

where

$$\tilde{W} = \tilde{\mathfrak{M}}_{\pi\pi}(b_3)\,\tilde{\mathfrak{R}}(b_2)\,\frac{e^{-z_1\sigma' T(b_1)/2} - e^{-z_2\sigma' T(b_1)/2}}{z_2 - z_1}\,,$$

and

$$z_1 = \frac{T(b_0)}{T(b_1)}\,,\quad z_2 = 1 + \frac{T(\vec{b}_1 + \vec{b}_2)}{T(b_1)} + \frac{T(\vec{b}_1 + \vec{b}_2 + \vec{b}_3)}{T(b_1)} - \frac{\sigma'}{8\pi a}\left[\frac{T(\vec{b}_1 + \frac{1}{2}\vec{b}_2)}{T(b_1)}\, e^{-b_2^2/4a} + \frac{T(\vec{b}_1 + \vec{b}_2 + \frac{1}{2}\vec{b}_3)}{T(b_1)}\, e^{-b_3^2/4a} + \frac{T(\vec{b}_1 + \frac{1}{2}\vec{b}_2 + \frac{1}{2}\vec{b}_3)}{T(b_1)}\, e^{-|\vec{b}_2 + \vec{b}_3|^2/4a}\right].$$

This expression reduces to Eq. (22) in the large-nucleus, small-γ (small-T) limit.

It should be emphasized that MIM is clearly different from the "spread-out A_1" model of Ref. 4, although both allow production outside the nucleus. A similar procedure to that of Ref. 4 would be to make the replacement in (9)

$$[1-\gamma(b_1)]^3 \to \int db_2\, db_3\, \tilde{F}_2(b_2)\,\tilde{F}_3(b_3)[1-\gamma(b_1)] \times [1-\gamma(\vec{b}_1 + \vec{b}_2)][1-\gamma(\vec{b}_1 + \vec{b}_2 + \vec{b}_3)]\,, \tag{30}$$

where $\tilde{F}_2(b_2)$ and $\tilde{F}_3(b_3)$ are some suitable transverse wave functions. A reasonable choice for $(\tilde{F}_2, \tilde{F}_3)$ is

$$(\tilde{F}_2(b_2), \tilde{F}_3(b_3)) = \left(\frac{\tilde{\mathfrak{R}}(b_2)}{\mathfrak{R}(q_2=0)}, \frac{\tilde{\mathfrak{M}}_{\pi\pi}(b_3)}{\mathfrak{M}_{\pi\pi}(q_3=0)}\right)\,, \tag{31}$$

and this yields a model with the structure

$$F_{3\pi C}^{G} = C\int d^2b_1\, e^{i\vec{q}_1\cdot\vec{b}_1} f^G(b_1)\,,$$

$$f^G(b_1) = \int d^2b_2\, d^2b_3\, \mathfrak{R}(q_2)\,\mathfrak{M}_{\pi\pi}(q_3)\,\frac{\tilde{\mathfrak{R}}(b_2)\,\tilde{\mathfrak{M}}_{\pi\pi}(b_3)}{\mathfrak{R}(0)\,\mathfrak{M}_{\pi\pi}(0)} \times G(b_1, b_2, b_3, b_0)\,, \tag{32}$$

$$G(b_1\, b_2\, b_3\, b_0) \equiv \frac{e^{-z_1\sigma' T(b_1)/2} - e^{-z_2\sigma' T(b_1)/2}}{z_2 - z_1}\,.$$

For comparison, MIM and SIM give the structures

$$\begin{aligned} f^{\text{SIM}}(b_1) &= \mathfrak{R}(q_2)\,\mathfrak{M}_{\pi\pi}(q_3)\, G(b_1, 0, 0, b_1) \\ &= \int d^2b_1\, d^2b_2\, e^{i(\vec{q}_2\cdot\vec{b}_2 + \vec{q}_3\cdot\vec{b}_3)} \times \tilde{\mathfrak{R}}(b_2)\,\tilde{\mathfrak{M}}_{\pi\pi}(b_3)\, G(b_1, 0, 0, b_1)\,, \\ f^{\text{MIM}}(b_1) &= \int d^2b_1\, d^2b_2\, e^{i(\vec{q}_2\cdot\vec{b}_2 + \vec{q}_3\cdot\vec{b}_3)} \times \tilde{\mathfrak{R}}(b_2)\,\tilde{\mathfrak{M}}(b_3)\, G(b_1, b_2, b_3, b_0)\,. \end{aligned} \tag{33}$$

It is clear that $f^G = f^{\text{MIM}}$ only in the special case that $G(b_1\, b_2\, b_3\, b_0) = G(b_1, 0, 0, b_1)$.

The detailed calculation of MIM is a formidable problem. Since $M_{\pi\pi}$ is small, $\mathfrak{M}_{\pi\pi}$ is dominated by resonance structure, and both $\tilde{\mathfrak{M}}_{\pi\pi}$ and $\tilde{\mathfrak{R}}$ must be considered as functions of more than one variable. The integrand of (29) is thus a function of all the kinematic variables describing 3π production. One might naively suppose that in the limit of very large nuclei, where $T(\vec{b}_1 + \vec{b}_i) \cong T(b)$, the effect of the Gaussian factors in z_2 would be to decrease the cross section, making the disagreement between theory and experiment even worse. However, γ is not small [for carbon $T(0) \approx 0.8$], and particles which pass near the center of a large nucleus will be strongly absorbed. Thus, the scattering process cannot be assumed to be dominated by regions of the nucleus where $T(b)$ is very slowly varying in b, no matter how large the nucleus.

Some information can be extracted from (29) and (33) by attempting to parametrize $f^{\rm MIM}(b_1)$ by an effective-pion number ($\bar{\Delta}$) which is a function of b_1,

$$f^{\rm MIM}(b_1, \vec{q}_2, \vec{q}_3) \cong \mathcal{R}(q_2)\,\mathfrak{M}_{\pi\pi}(q_3)\,\frac{e^{-\sigma' T(b_1)/2} - e^{-\bar{\Delta}(b_1)\sigma' T(b_1)/2}}{\bar{\Delta}(b_1) - 1}\,. \tag{34}$$

The approximate equality is because the $(\vec{q}_2, \vec{q}_3)$ dependence of $f^{\rm MIM}$ in (33) is more complicated than in (34). One hopes, however, that the dependence of $\bar{\Delta}(b_1)$ on $(\vec{q}_2, \vec{q}_3)$ will be weak, and that a suitable average may be taken in these variables.

A simple Gaussian form is used for $\tilde{\mathcal{R}}$ and $\tilde{\mathfrak{M}}_{\pi\pi}$:

$$\tilde{\mathcal{R}}(b) = \tilde{\mathfrak{M}}_{\pi\pi}(b) = e^{-b^2/2a}\,,$$
$$\mathfrak{M}_{\pi\pi}(q) = \mathcal{R}(q) = 2\pi a\, e^{-aq^2/2}\,, \tag{35}$$
$$a = 8\ {\rm GeV}^{-2}\,.$$

This parametrization is reasonably consistent with the momentum transfer distribution in the Deck calculation of $\pi p \to 3\pi p$. After choosing values of $\vec{q}_2$ and $\vec{q}_3$, these forms are used in (33) to evaluate $f^{\rm MIM}(b_1)$, performing the 4-dimensional integral numerically. For each value of b_1, (34) is solved graphically for $\bar{\Delta}(b_1)$, which is assumed to be real. The results of this calculation are shown in Fig. 6, where the shaded region shows the range of $\bar{\Delta}(b_1)$ that was obtained by four choices of $\vec{q}_2$ and $\vec{q}_3$. The actual range of $\bar{\Delta}(b_1)$ is presumably somewhat greater than the region shown. The SIM value for Δ, calculated by substituting $G(b_1, b_2, b_3, b_0) \to G(b_1, 0, 0, b_1)$ in $\bar{\Delta}(b)$, is shown in Fig. 6 as a dashed line at $\Delta = 2.20$. This differs slightly from the previous value of Δ because of the approximations used in evaluating $\bar{\Delta}(b_1)$.

The quantity Δ in (22) may now be made a function of b_1 using typical values of $\bar{\Delta}(b)$, and $Z(t)$

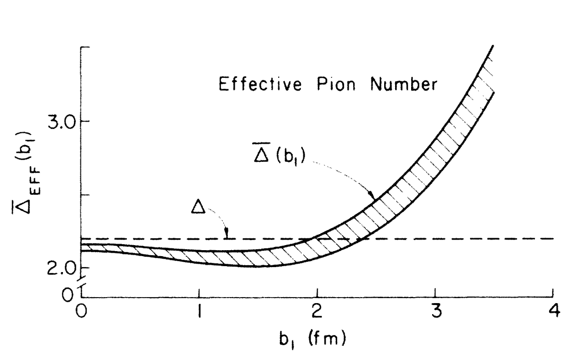

FIG. 6. Effective pion number $\bar{\Delta}(b_1)$ for the multi-impact-parameter model (MIM).

calculated as in Sec. III. The result is found to be less than 1% larger than the SIM result [curve (b)] of Fig. 2 at $t = 0$. Although a more detailed calculation might yield slightly different results, it seems clear that cross sections calculated with the multi-impact-parameter model will not differ appreciably from those calculated using the more conventional single-impact-parameter model.

V. THE PRODUCTION OF $C^*_{4.44}$

Glauber theory can be used to calculate $\pi C \to \pi C^*$ and $\pi C \to 3\pi C^*$ by making the substitution in (1) and (8)

$$|u(\vec{r}_1, \ldots, \vec{r}_A)|^2 \to u_f^*(\vec{r}_1, \ldots, \vec{r}_A)u_i(\vec{r}_1, \ldots, \vec{r}_A)\,. \tag{36}$$

The problem now becomes one of finding a suitable form for $u_f^* u_i$. The simplest approach is to use an effective one-particle excitation for the excited state of the nucleus. For $A = 2$, and denoting the excited orbital by $\bar{\phi}$,

$$\begin{aligned}
u_i &= \left(\frac{1}{2!}\right)^{1/2}[\phi_1(\vec{r}_1)\,\phi_2(\vec{r}_2) - \phi_1(\vec{r}_2)\,\phi_2(\vec{r}_1)]\,,\\
u_f &= \left(\frac{1}{2!}\right)^{1/2}[\bar{\phi}_1(\vec{r}_1)\,\phi_2(\vec{r}_2) - \bar{\phi}_1(\vec{r}_2)\,\phi_2(\vec{r}_1)]\,,\\
u_f^* u_i &= \frac{1}{2!}\,[\bar{\phi}_1^*(\vec{r}_1)\,\phi_1(\vec{r})\,\phi_2^*(\vec{r}_2)\,\phi_2(\vec{r}_2)\\
&\qquad - \bar{\phi}_1^*(\vec{r}_1)\,\phi_1(\vec{r}_2)\,\phi_2^*(\vec{r}_2)\,\phi_2(\vec{r}_1) + (\vec{r}_1 \leftrightarrow \vec{r}_2)]\,,\\
&= \frac{1}{2!}\,[\bar{\rho}_1(\vec{r}_1)\rho_2(\vec{r}_2) + \bar{\rho}_1(\vec{r}_2)\rho_2(\vec{r}_1)\\
&\qquad + (\text{correlation terms})]\,.
\end{aligned} \tag{37}$$

This is easily generalized to

$$u_f^*(\vec{r}_1, \ldots, \vec{r}_A)u_i(\vec{r}_1, \ldots, \vec{r}_A) \cong \frac{1}{A}\sum_{i=1}^{A}\bar{\rho}(r_i)\prod_{l\neq i}\rho(r_l)\,. \tag{38}$$

As in (3), correlation terms have been dropped. This is expected to be a rather poor description of $C^*_{4.44}$, which is well known to be a state with collective properties,[15] and should be considered as a parametrization rather than an actual excitation mechanism.

Electron scattering data are often used to determine $\bar{\rho}$. In the case of $eC \to eC^*$, the weakness of the electromagnetic interaction ensures that one-particle operators dominate, and matrix elements with multiparticle correlation terms are down by powers of α. The multiple scattering of an incident pion, however, is significant. In fact, in (7) and (22) the entire multiple-scattering series has been summed. It thus seems more reasonable, if one wishes to calculate $\pi C \to 3\pi C^*$, to determine $\bar\rho$ from $\pi C \to \pi C^*$ than from $eC \to eC^*$. Using

$$1=\int \rho(\vec{r})\,d^3r\,,\quad 0=\int \bar\rho(\vec{r})\,d^3r\,,\quad T(b)\equiv A\int \rho(\vec{b},z)\,dz\,,\quad \bar T_M(\vec{b})\equiv A\int \bar\rho_M(\vec{b},z)\,dz\,, \tag{39}$$

with M labeling the spin projection of the $J=2$ final state of the nucleus, one finds by summation of the Glauber series

$$\begin{aligned} F^M_{\pi C^*} &= \frac{ik}{2\pi}\int d^2b\left(\prod_k d^3r_k\right)e^{i\vec{q}\cdot\vec{b}}\left[\frac{1}{A}\sum_{i=1}^{A}\bar\rho_M(r_i)\prod_{l\neq i}\rho(r_l)\right]\left\{1-\prod_{m=1}^{A}[1-\Gamma(\vec{b}-\vec{s}_m)]\right\},\\ &= \frac{ik}{2\pi}\int d^2b\,e^{i\vec{q}\cdot\vec{b}}\left(\frac{e^{-\sigma' T(b)/2}}{1-\sigma' T(b)/2A}\right)\frac{\sigma'\bar T_M(\vec{b})}{2A}. \end{aligned} \tag{40}$$

This formula is essentially the same as that of Ravenhall and Schult.[16]

The Glauber amplitude for $\pi C\to 3\pi C^*$ is, then,

$$\begin{aligned} F^M_{3\pi C^*} = \frac{ik}{2\pi}\sum_{j=1}^{A}\int d^2b\left(\prod_{k=1}^{A}d^3r_k\right)e^{i\vec{q}\cdot\vec{b}}\left[\frac{1}{A}\sum_{m=1}^{A}\bar\rho_M(\vec{r}_m)\prod_{n\neq m}\rho(r_n)\right]e^{iq_L z_j}\,\Gamma_{\pi,3\pi}(\vec{b}-\vec{s}_j)\prod_{z_i<z_j}[1-\gamma(\vec{b}-\vec{s}_i)]\\ \times\prod_{z_l>z_j}[1-\Gamma_{3\pi,3\pi}(\vec{b}-\vec{s}_l)]\,. \end{aligned} \tag{41}$$

Of the A nucleons, there are now two of special interest: There is the excited nucleon and the nucleon on which 3π production occurs. If the excited nucleon is on the beam side of the production site, it sees one pion; if to the downstream side, three pions. Of course, the excited nucleon may in fact be the production nucleon. So the sums in (41) will have three contributions.

Since this formalism will be used at 6 GeV/c, q_L will not be assumed small. Using the same approximations as in the derivation of (22), and with

$$\begin{aligned} &T(b,q_L)\equiv A\int \rho(b,z)\,e^{iq_L z}\,dz\,,\\ &\bar T_M(b,q_L)\equiv A\int \bar\rho_M(b,z)\,e^{iq_L z}\,dz\,,\\ &x\equiv 1-\frac{\sigma' T(b)}{2A}\,,\quad \bar x\equiv 1-\frac{\sigma'\bar T_M(\vec{b})}{2A}\,,\\ &y\equiv 1-\Delta\frac{\sigma' T(b)}{2A}\,,\quad R\equiv\frac{T(b,q_L)}{T(b)}\,,\quad \bar R_M\equiv\frac{\bar T_M(b,q_L)}{\bar T_M(b)}\,, \end{aligned} \tag{42}$$

the scattering amplitude becomes

$$F^M_{3\pi C^*}=\frac{i\sqrt2}{(2\pi)^4\,2^3}\left(\frac{p_{3\pi}^{\mathrm{c.m.}}}{p_\pi}\right)^{1/2}\sum_{\mathrm{diagrams}}\left(\frac{p_{\pi N}^{\mathrm{c.m.}}M_{\pi N}}{M_N}\right)\mathfrak{M}_{\pi\pi}\mathfrak{R}\bar Z_M(\vec{q}_\perp,q_L)\,, \tag{43}$$

where

$$\begin{aligned} \bar Z_M(\vec{q}_\perp,q_L)=\int d^2b\,e^{i\vec{q}_\perp\cdot\vec{b}}\,\frac{1}{A}\Bigg[&-\left(\frac{\sigma' T(b)}{2A}\right)\left(\frac{\sigma'\bar T_M(b)}{2A}\right)R\sum_{j=1}^{A-1}j(\Delta\,x^{A-1-j}y^{j-1}+x^{j-1}y^{A-1-j})\\ &+\left(\frac{\sigma'\bar T_M(b)}{2A}\right)\bar R_M\sum_{j=1}^{A}x^{A-j}y^{j-1}\Bigg]\,. \end{aligned}$$

Summing the series and using (6), one finds

$$\begin{aligned} \bar Z_M(\vec{q}_\perp,q_L)=\int d^2b\,e^{i\vec{q}_\perp\cdot\vec{b}}\,\frac{\sigma'\bar T_M(\vec{b})}{2A}\left(\frac{1}{\Delta-1}\right)\Bigg[&R\left(\frac{\Delta e^{-\Delta\sigma' T(b)/2}}{1-\Delta\sigma' T(b)/2A}-\frac{e^{-\sigma' T(b)/2}}{1-\sigma' T(b)/2A}\right)\\ &+(\bar R-R)\left(\frac{e^{-\sigma' T(b)/2}-e^{-\Delta\sigma' T(b)/2}}{\sigma' T(b)/2}\right)\Bigg]\,. \end{aligned} \tag{44}$$

An interesting fact is that for $q_L=0$ ($\bar R=R=1$) the second term in (44) vanishes. This means that the term originating from the C* being formed by exciting the same nucleon that 3π production takes place on is canceled by part of the amplitude corresponding to excitation and production occurring at different sites. This interesting cancellation is a feature peculiar to the Deck model, arising from the fact that the lower vertex of the Deck amplitude ($\mathfrak{M}_{\pi N}$) is the same as the interaction that causes absorption. The cross section for $3\pi C^*$ production is given by

$$d\sigma = \frac{1}{(2\pi)^8 2^6} \times \sum_{M=-2}^{2} \left| \sum_{\text{diagrams}} \left(\frac{p_{\pi N}^{\text{c.m.}} M_{\pi N}}{p_\pi M_N} \right) \mathfrak{M}_{\pi\pi} \mathfrak{R} \bar{Z}_M(\vec{q}_\perp, q_L) \right|^2 d^8\tau \,. \qquad (45)$$

To calculate $\bar{T}_M(b)$, the excitation form factor may be parametrized by

$$\bar{\rho}_M(\vec{r}) = \frac{2C}{\sqrt{5}\,\pi \bar{r}_0^{\,5}} r^2 e^{-r^2/\bar{r}_0^2} Y_{2M}(\theta, \phi) \,, \qquad (46)$$

where the angles are referred to the recoil direction of the nucleus ($\hat{Z}$). If $\hat{Y}$ is perpendicular to the scattering plane, and $\hat{X} \equiv \hat{Y} \times \hat{Z}$, then Cartesian combinations of the $\bar{\rho}_M$ are

$$\bar{\rho}_0 = \bar{\rho}_0 \sim \frac{1}{\sqrt{6}} (2Z^2 - X^2 - Y^2) \,,$$

$$\bar{\rho}_{1+} = \frac{1}{\sqrt{2}} (\bar{\rho}_1 + \bar{\rho}_{-1}) \sim -\sqrt{2}\, iYZ \,,$$

$$\bar{\rho}_{1-} = \frac{1}{\sqrt{2}} (\bar{\rho}_1 - \bar{\rho}_{-1}) \sim \sqrt{2}\, XZ \,, \qquad (47)$$

$$\bar{\rho}_{2+} = \frac{1}{\sqrt{2}} (\bar{\rho}_2 + \bar{\rho}_{-2}) \sim \frac{1}{\sqrt{2}} (X^2 - Y^2) \,,$$

$$\bar{\rho}_{2-} = \frac{1}{\sqrt{2}} (\bar{\rho}_2 - \bar{\rho}_{-2}) \sim \sqrt{2}\, iXY \,.$$

By symmetry, $\bar{\rho}_{1+}$ and $\bar{\rho}_{2-}$ give zero contribution when the Y integration in (44) is performed.

VI. CALCULATION OF $\pi^- C \to \pi^+ \pi^- \pi^- C^*_{4.44}$

Experimental $\pi C \to \pi C^*$ data at 4.5 GeV/c (see Ref. 17) and 3 GeV/c (see Ref. 18) were analyzed using (40) and (46). The shape of the experimental t distribution is well reproduced by $\bar{r}_0 = 1.77$ fm, and the normalization gives $C = 3.19 \pm 0.02$. Theoretical curves for $\pi C \to \pi C^*$ are shown in Fig. 7. The experimental data will appear in Ref. 17. Equation (44) is now used to calculate ($\bar{Z}_0, \bar{Z}_{1-}, \bar{Z}_{2+}$), and the result is shown in Fig. 8 for two values of q_L. For $q_L = 0$, the 2+ contribution is greater than it is in $\pi C \to \pi C^*$, when compared to the $M = 0$ contribution. For $q_L = 0.1$ GeV, which is a typical value near the peak of the $M_{3\pi}$ distribution, $M = 0$ is seen to dominate strongly.

The next step is to perform a Monte Carlo calculation of (45) at incident pion momentum 6 GeV/c, in order to compare with the experimental results of Ref. 9. The low-pion momentum adversely affects the validity of an approximation that has been made throughout this research. A

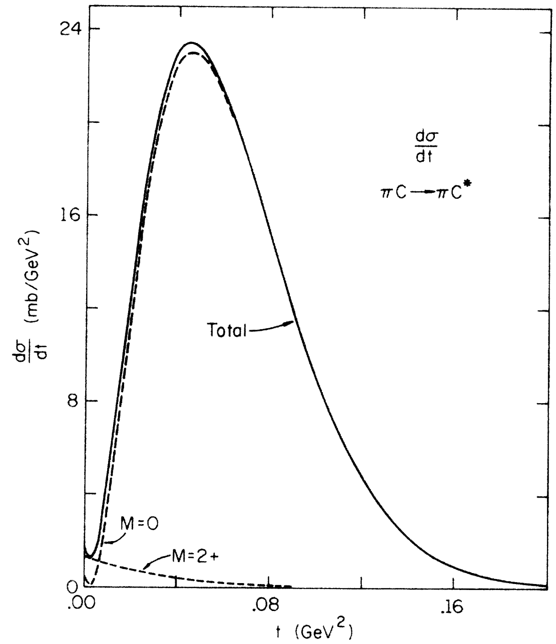

FIG. 7. Calculated cross section for $\pi C \to \pi C^*_{4.44}$. M is the helicity of the C*.

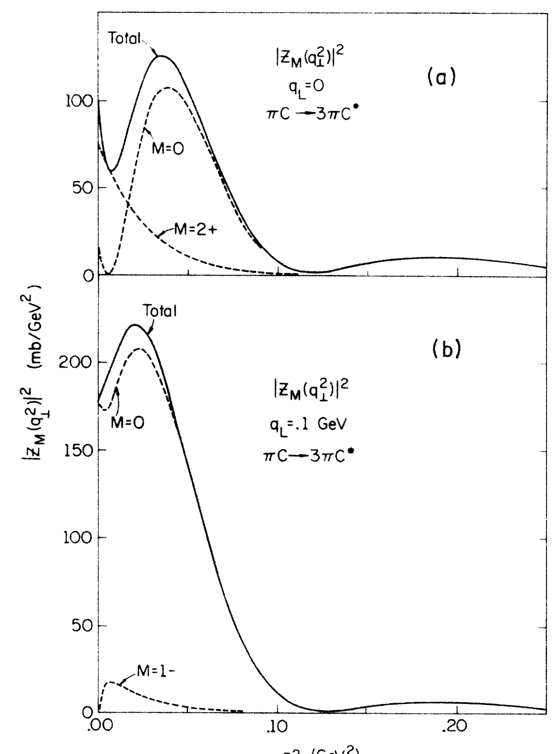

FIG. 8. $|\bar{Z}_M(q_\perp, q_L)|^2$ for $\pi^- C \to \pi^+\pi^-\pi^- C^*_{4.44}$, in the independent-pion final-state model ($\Delta = 2.17 - 0.14i$). M is the helicity of the C*.

significant fraction of events has $M_{\pi C}$ in the resonance region, $M_{\pi N} \lesssim 1.5$ GeV, and the approximation that $\gamma(b)$ is energy-independent underestimates the interaction in this region. The effect may be estimated by comparing, in I, the results of FIT 1, which uses experimental $\pi C \to \pi C^*$ data for the resonance region, and FIT 3, which uses an energy-independent πC interaction. FIT 1 yields a $3\pi C^*$ cross section 15% higher than FIT 3, and the calculation performed here may be expected to be too small by a similar amount. This effect is negligible at 15.1 GeV/c incident momentum.

Since the data of Ref. 9 have not as yet been analyzed to yield a value of $\sigma_{3\pi}$, the Monte Carlo calculation was performed both with the value of Δ appropriate to the independent pion final-state model ($\Delta = 2.17 - 0.14i$) and the value of Δ which seems to fit the $\pi C \to 3\pi C$ data ($\Delta = 1.1$). About 25 000 events with $0.8 < M_{3\pi} < 1.8$ GeV were generated for each value of Δ. Figure 9 shows $d\sigma/dM_{3\pi}$, along with the experimental results from Ref. 9. These experimental data have been corrected for spectrometer acceptance. The shapes of the $M_{3\pi}$ spectra for both values of Δ are consistent with experiment, and are virtually identical with the $M_{3\pi}$ spectra in I.

The cross section[19] for $3\pi C^*$ production with $0.8 < M_{3\pi} < 1.4$ GeV is 76 μb in the independent pion model and 126 μb for $\Delta = 1.1$. Current analysis of experimental $\pi C \to 3\pi C^*$ data at 6 GeV/c yields a preliminary cross section[20] of 130 μb for the same range of $M_{3\pi}$. Although this cross section may be affected by future refinements in the calculation of experimental acceptances, its present value is clearly more consistent with the $\Delta = 1.1$ cross section than the $\Delta = 2.17 - 0.14i$ value.

It should be mentioned that $d\sigma/dM_{3\pi}$ for $\Delta = 1.1$ is virtually identical to the result of FIT 3 in I. This would not be surprising if as Δ approached unity, $\overline{Z}_M$ were to become proportional to $F^M_{\pi C^*}$. In this case the two models would be formally identical. Unfortunately, $\overline{Z}_M(\Delta \to 1)$ has a very different structure from $F^M_{\pi C^*}$. It is not clear what causes the agreement in $d\sigma/dM_{3\pi}$ between the two models.

The shape of the experimental t distribution is analyzed in some detail in Ref. 9. To this end, the normalization of the theoretical distribution in $q_\perp^2$ is fitted to the data presented in Ref. 9, and the results are shown in Fig. 10. The last three data bins ($q_\perp^2 > 0.09$ GeV^2) have been dropped from the fit, and a spectrometer acceptance[21] of $(1 - 1.36\, q_\perp^2)$ is multiplied into the theoretical curves. The fit has confidence level 0.002 for $\Delta = 2.17 - 0.14i$, and 0.65 for $\Delta = 1.1$. The shape of the $q_\perp^2$ distribution is clearly more consistent with $\Delta = 1.1$ than with the independent-pion model.

The density matrix $\rho_{mm'}$, where m is the helicity[22] of the C*, can be extracted from the Monte Carlo calculation. Table I shows $\rho_{mm'}$ integrated over all kinematic variables in the range $0.8 < M_{3\pi} < 1.4$ GeV.

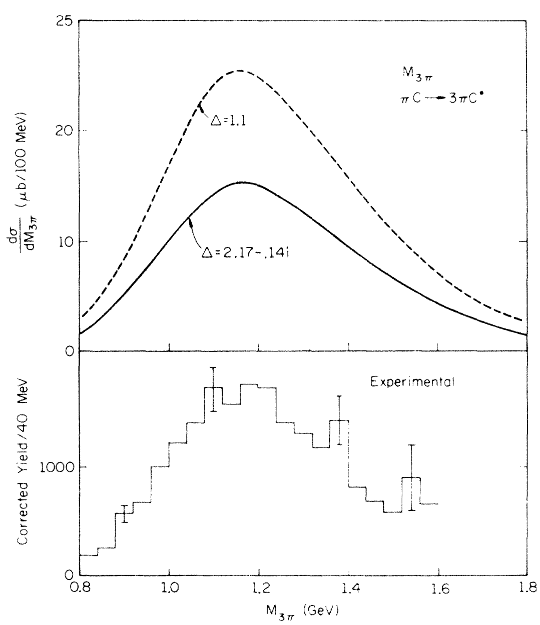

FIG. 9. 3π mass spectrum for $\pi^- C \to \pi^+\pi^-\pi^- C^*_{4.44}$. Experimental curve is from Ref. 9. $\Delta = 2.17 - 0.14i$ is the independent-pion final-state model.

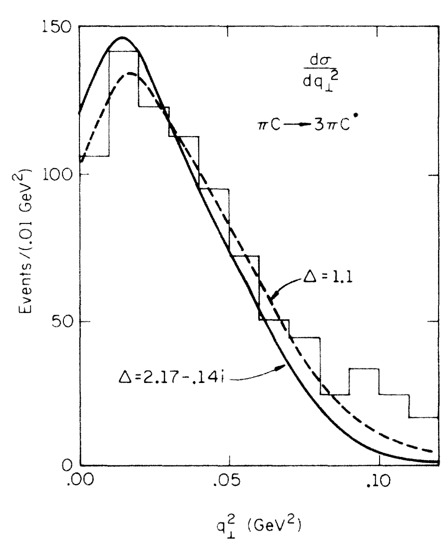

FIG. 10. Distribution in $q_\perp^2$ for $\pi^- C \to \pi^+\pi^-\pi^- C^*_{4.44}$. The normalization of the theoretical curves has been fitted to the experimental data. Experimental curve from Ref. 9. $\Delta = 2.17 - 0.14i$ is the independent-pion final-state model.

TABLE I. Density matrix $\rho_{mm'}$ integrated over 0.8 $<M_{3\pi}<1.4$ GeV.

	0,0	1−,1−	2+,2+	0,1−	0,2+	1−,2+
$\Delta=2.17-0.14i$	0.957	0.029	0.014	−0.13	0.09	−0.02
$\Delta=1.1$	0.970	0.019	0.011	−0.11	0.08	−0.01

VII. CONCLUSION

It has been shown in this paper that, for the reaction $\pi C\to 3\pi C$, neither calculating realistically in all the kinematic variables of a Deck production mechanism nor allowing for reduced ρ absorption nor using a multi-impact-parameter model will substantially affect the conclusion that a three-independent-pion final state in the Glauber picture of 3π production gives cross sections which are inconsistent with experiment. Glauber theory does describe this reaction reasonably well if the effective-pion number, Δ, of the final state is taken to be about 1.1.

The reaction $\pi C\to 3\pi C^*$ has been calculated, again using Glauber theory as well as a simple excitation parametrization. The results of the calculation are again inconsistent with experiment if one uses an independent-final-pion model, but seem to agree very well with the data if $\Delta=1.1$. The same value of effective-pion number seems to be indicated in both $\pi C\to 3\pi C$ and $\pi C\to 3\pi C^*$.

ACKNOWLEDGMENTS

I would like to thank Professor H. W. Wyld for many informative discussions and for his guidance and support. I would also like to thank Professor R. L. Schult for his extremely helpful comments and information.

APPENDIX

The starting points of the Glauber theories presented [Eqs. (1), (8), and (26)] are here derived pedagogically. The method used, which was demonstrated to me by Schult, may be well known in some quarters, although we do not know of its being published previously. It is not intended to be a rigorous derivation.

The point of this exercise is to keep track of the phase accumulated by each particle as it propagates from nucleon to nucleon, in order to find the outgoing scattered wave function ψ_0. A projection will then be taken on plane-wave outgoing states. This process is intended to reproduce the structure of the desired answers, and will ignore details like kinematic factors.

Elastic scattering illustrates the basic features of this method. The outgoing scattered wave function for $\vec{k}_{in}=k_{in}\hat{z}$ is, in the small-angle approximation,

$$\begin{aligned}\psi_0(\vec{r}) &= \exp[i\vec{k}_{in}\cdot\vec{r}_1+2i\delta_1+i\vec{k}_{in}\cdot(\vec{r}_2-\vec{r}_1)\\ &\quad +2i\delta_2+\cdots+i\vec{k}_{in}\cdot(\vec{r}_A-\vec{r}_{A-1})\\ &\quad +2i\delta_A+i\vec{k}_{in}\cdot(\vec{r}-\vec{r}_A)]-\exp(i\vec{k}_{in}\cdot\vec{r})\\ &= \exp\left(i\vec{k}_{in}\cdot\vec{r}+\sum_{l=1}^{A}2i\delta_l\right)-\exp(i\vec{k}_{in}\cdot\vec{r}),\end{aligned} \tag{A1}$$

$$e^{2i\delta_l}=e^{2i\delta(\vec{b}-\vec{s}_l)}=1-\gamma(\vec{b}-\vec{s}_l),$$

where $\vec{r}_i=(\vec{b}_i,z_i)$ is a nucleon position and $\delta_l=\delta(\vec{b}-\vec{s}_l)$ is a phase shift on the lth nucleon. Projecting ψ_0 into a plane-wave state $e^{i\vec{k}_0\cdot\vec{r}}$, and taking a matrix element between nuclear states,

$$\begin{aligned}F_{\pi C} &= \left\langle \text{nucl}\left|\int d^3r\, e^{-i\vec{k}_0\cdot\vec{r}}\,\psi_0(\vec{r})\right|\text{nucl}\right\rangle\\ &= 2\pi\delta(k_{in\,z}-k_{0z})\\ &\quad\times\int d^2b\, e^{i\vec{q}\cdot\vec{b}}\left\langle\text{nucl}\left|\left\{\prod_l[1-\gamma(b-s_l)]-1\right\}\right|\text{nucl}\right\rangle,\end{aligned} \tag{A2}$$

which is essentially equivalent to (1).

Equation (8) may be derived in a similar way by assuming that the longitudinal transfer to momentum all occurs at the nucleon where (3π) production takes place. Then, if production occurs on the jth nucleon,

$$\begin{aligned}\psi_0 &= \exp[i\vec{k}_{in}\cdot\vec{r}_1+2i\delta_1+\cdots+i\vec{k}_{in}\cdot(\vec{r}_j-\vec{r}_{j-1})]\,\Gamma_{\pi,3\pi}(\vec{b}-\vec{s}_j)]\exp[i\vec{k}'\cdot(\vec{r}_{j+1}-\vec{r}_j)+2i\delta'_{j+1}+\cdots+i\vec{k}'\cdot(\vec{r}-\vec{r}_A)]\\ &= e^{i\vec{k}'\cdot\vec{r}}\prod_{i=1}^{j-1}e^{2i\delta_j}\,\Gamma_{\pi,3\pi}(\vec{b}-\vec{s}_j)\prod_{l=j+1}^{A}e^{2i\delta'_l}\,e^{iq_Lz_j},\end{aligned} \tag{A3}$$

where

$$\vec{k}'\equiv(k_{in}-q_L)\hat{z}=(\vec{k}_0\cdot\hat{z})\hat{z},$$

$$e^{2i\delta'_l}=[1-\Gamma_{3\pi,3\pi}(\vec{b}-\vec{s}_l)].$$

As before,

$$F_{3\pi A} = \left\langle \text{nucl} \left| \int d^3r\, e^{-i\vec{k}_0\cdot\vec{r}}\, \psi_0 \right| \text{nucl} \right\rangle$$

$$= 2\pi\delta(\vec{k}_0\cdot\hat{z} - k')\int d^2b\, e^{i\vec{q}\cdot\vec{b}} \sum_j \left\langle \text{nucl} \left| \prod_{z_i<z_j} [1-\gamma(\vec{b}-\vec{s}_i)]\, e^{iq_L z}\, \Gamma_{\pi,3\pi}(\vec{b}-\vec{s}_j) \prod_{z_l>z_j} [1-\Gamma_{3\pi,3\pi}(\vec{b}-\vec{s}_l) \right| \text{nucl} \right\rangle , \tag{A4}$$

which is equivalent to (8).

The MIM formalism is derived in exactly the same way, although there are many more variables in this case. Defining $(\vec{k}_1, \vec{k}_2, \vec{k}_3)$ to be the momenta of the three pions with $(\vec{r}', \vec{r}'', \vec{r}''')$ the space variables conjugate to the $\vec{k}_i$, one writes

$$\psi_0(\vec{r}) = \exp[i\vec{k}_{in}\cdot\vec{r}_1 + 2i\delta_1 + \cdots + i\vec{k}_{in}\cdot(\vec{r}_j - \vec{r}_{j-1})\,\Gamma_{\pi,3\pi}(b_1, b_2, b_3)]\exp[i\vec{k}_1'\cdot(\vec{r}_{j+1}-\vec{r}_j) + 2i\delta'_{j+1} + \cdots + i\vec{k}_1'\cdot(\vec{r}'-\vec{r}_A)]$$

$$\times\exp[i\vec{k}_2'\cdot(\vec{r}_{j+1}-\vec{r}_j) + 2i\delta''_{j+1} + \cdots + i\vec{k}_2'\cdot(\vec{r}''-\vec{r}_A)]\exp[i\vec{k}_3'\cdot(\vec{r}_{j+1}-\vec{r}_j) + 2i\delta'''_{j+1} + \cdots + i\vec{k}_3'\cdot(\vec{r}'''-\vec{r}_A)],$$

$$\vec{k}_1' = (\vec{k}_1\cdot\hat{z})\hat{z}, \quad k_2' = (\vec{k}_2\cdot\hat{z})\hat{z}, \quad k_3' = (\vec{k}_3\cdot\hat{z})\hat{z}.$$

A moderate amount of algebra will result in (26).

---

*Work supported in part by the National Science Foundation under Grant No. NSF GP 40908X and in part by the U. S. Atomic Energy Commission under Grant No. AT(11-1)-1195.

[1]J. S. Trefil, Phys. Rev. Lett. 23, 1075 (1969).
[2]C. Bemporad *et al.*, Nucl. Phys. B42, 627 (1972).
[3]C. Bemporad *et al.*, Nucl. Phys. B33, 397 (1971).
[4]A. Goldhaber *et al.*, Phys. Rev. Lett. 22, 802 (1969).
[5]P. M. Fishbane *et al.*, Phys. Lett. 41B, 153 (1972).
[6]For a complete list of references see Ref. 7.
[7]G. Ascoli *et al.*, Phys. Rev. D 9, 1963 (1974); G. Ascoli *et al.*, *ibid.* 8, 3894 (1973); E. L. Berger, Phys. Rev. 166, 1525 (1968).
[8]A few of the many papers on or related to this topic are as follows: L. Van Hove, Nucl. Phys. B46, 75 (1972); CERN Report No. TH. 1685, 1973 (unpublished); K. Gottfried, CERN Report No. TH. 1735, 1973 (unpublished); A. Bialas and K. Zalewski, Cracow Report No. TPJU-2173, 1973 (unpublished); A. Białas, W. Czyż, and A. Kotański, Ann. Phys. (N.Y.) 73, 439 (1972); W. Czyż, Phys. Rev. D 8, 3219 (1973); J. Pumplin, *ibid.* 8, 2899 (1973); W. Czyż, Ann. Phys. (N.Y.) 52, 59 (1969).
[9]G. Ascoli *et al.*, Phys. Rev. Lett. 31, 795 (1973).
[10]R. Cutler, Phys. Rev. D 9, 676 (1974). This reference is referred to as I in the text.
[11]R. J. Glauber, in *Lectures in Theoretical Physics*, edited by W. E. Britten *et al.* (Interscience, New York, 1959), Vol. 1, p. 315; in *High Energy Physics and Nuclear Structure*, edited by G. Alexander (North-Holland, Amsterdam, 1967), p. 311.
[12]S. Kölbig and B. Margolis, Nucl. Phys. B6, 85 (1968).
[13]H. Ehrenberg *et al.*, Phys. Rev. 113, 666 (1959).
[14]R. Spital and D. Yennie, Phys. Rev. D 9, 138 (1974).
[15]G. Morpurgo, Nuovo Cimento 3, 430 (1956); H. Überall, *Electron Scattering from Complex Nuclei, Part B* (Academic, New York, 1971).
[16]R. L. Schult (private communication). This theory is presented and used to analyze the experiment of Ref. 17.
[17]J. L. Groves, L. E. Holloway, L. J. Koester, W. K. Liu, L. J. Nodulman, D. G. Ravenhall, J. H. Smith, and R. L. Schult (unpublished).
[18]D. Scipione *et al.*, Phys. Lett. 42B, 489 (1972).
[19]The effects of resonance production and numerical approximations have been estimated by adding 20% to the total cross sections. This factor has not been included in the figures.
[20]I would like to thank U. Kruse and B. Wojslaw for allowing me to quote this cross section.
[21]R. Wojslaw (private communication).
[22]Another representation of $\rho_{mm'}$ is $\rho_{1,1} = \frac{1}{2}\rho_{1-,1-}$, $\rho_{2,2} = \frac{1}{2}\rho_{2+,2+}$, $\rho_{0,2} = 2^{-1/2}\rho_{0,2+}$, $\rho_{0,1} = 2^{-1/2}\rho_{0,1-}$, $\rho_{1,2} = \frac{1}{2}\rho_{1-,2+}$, $\rho_{1,-1} = -\rho_{1,1}$, $\rho_{1,-2} = \rho_{1,2}$, $\rho_{2,-2} = \rho_{22}$.